2R.8

HIGH-RESOLUTION OBSERVATIONS OF DYNAMIC STRUCTURES IN THE BOUNDARY LAYER USING A RANGE IMAGING WIND PROFILER AND AN FMCW RADAR

Phillip B. Chilson[1], James R. Jordan[2], and Scott A. McLaughlin[3]
[1] University of Oklahoma, Norman, Oklahoma
[2] NOAA Environmental Technology Laboratory, Boulder, Colorado
[3] Applied Technologies, Inc., Longmont, Colorado

1 Introduction

Boundary layer radars (BLRs) are widely and successfully used to study and monitor the lowest reaches of the atmosphere. The term BLR is generally used to describe a class of pulsed Doppler radar that transmits radio waves vertically or near vertically and receives backscattered signals from the refractive-index fluctuation of the optically clear atmosphere. Profiles of the wind vector directly above the instrument are obtained using the Doppler beam swinging (DBS) method [Balsley and Gage, 1982]. Since they typically operate at a frequency near 1 GHz, BLRs are also sensitive to Rayleigh scatter from hydrometeors and are also used to study clouds and precipitation [Gage et al., 1994; Ecklund et al., 1995]. That is, the BLR can be used to study the boundary layer under a wide variety of meteorological conditions [e.g., Rogers et al., 1993; Angevine et al., 1994; Wilczak et al., 1996; Dabberdt et al., 2004].

By way of example, one important application of BLRs is for the study of the evolution of the convective boundary layer (CBL). BLRs have been widely used to estimate the depth of the CBL and thickness of the entrainment layer [e.g., Angevine et al., 1994; Angevine, 1999; Cohn and Angevine, 2000; Grimsdell and Angevine, 2002]. Enhanced refractive index variations are often associated with the entrainment zone just above the CBL, which can be detected by clear-air radar. Unfortunately, BLRs must operate within stringent frequency management constraints, which limit their range resolution. A typical range resolution for BLR measurements of the atmospheric boundary layer is about 100 m, which is too coarse to adequately reproduce the spatial structure embedded within the entrainment zone. Range imaging (RIM) has been recently developed as a means of improving range resolution [Palmer et al., 1999] and has furthermore been shown to be effective for measurements within the boundary layer at UHF [Chilson et al., 2003].

[1] *Corresponding author address:* Phillip B. Chilson, School of Meteorology, University of Oklahoma, Norman, OK, 73019-1000

2 Range Imaging

In order to overcome range resolution limitations imposed on wind profiling radars, a frequency hopping technique known as RIM has been developed [Palmer et al., 1999]. In this technique, several closely spaced carrier frequencies are transmitted and received, and a constrained optimization method is used to generate high-resolution maps of the reflectivity field in range. The fundamentals of RIM are analogous to the principles of beam forming used in coherent radar imaging (CRI) [Woodman, 1997; Palmer et al., 1998; Hysell, 1996; Chau and Woodman, 2001; Yu and Palmer, 2001]. Whereas CRI uses radar signals from multiple receive antennas to image in angle, in RIM different radar frequencies are used to image in range.

The Doppler radar signal from N radar frequencies are represented as $s_n(t)$, where t is time and $n = 1 \ldots N$. As described in Palmer et al. [1999], a composite (or synthesized) Doppler radar signal is created using the weighted sums of the original data through the equation

$$\tilde{s}_j(t) = \sum_{n=1}^{N} w_{jn} s_n(t), \qquad (1)$$

Typically, one creates a set of evenly spaced val-

ues in a range for which the weighting vector, $\mathbf{w}$, should be calculated. The values w_{jn} are expressed collectively as $\mathbf{w}$. And the collective set of range values is referred to as *subgates*. These are indexed by j in (1). The expression $\tilde{s}_j(t)$ is referred to as the synthesized Doppler radar signal. Note that $\mathbf{w}$ must be calculated for each time step t.

The task of finding a weighting matrix such that the sensitivity of the radar is focused at a specific range is one of a mathematical inversion problem. Essentially, it is desired to adjust the phase and/or amplitude of the Doppler radar signals in such a way as to produce constructive interference at the desired location in space. Many algorithms have been proposed in order to achieve this task [Palmer et al., 1999; Luce et al., 2001; Yu and Palmer, 2001; Smaïni et al., 2002]. It has recently been shown that RIM can be successfully applied at UHF for studies of the boundary layer [Chilson et al., 2003]. In addition to measurements of the reflectivity, RIM can also be used to improve the range resolution of radar wind measurements [Chilson, 2004].

Once the synthesized Doppler radar signal as given in (1) has been found, the Doppler moments are found in the usual way by calculating the Doppler spectra. That is, it is possible to obtain the backscattered power (zeroth moment), the radial velocity (first moment), and the spectral width (second central moment). However, these moments can now be calculated for each of the chosen subgates (subset of the nominal range resolution).

3 Experiment

A RIM validation experiment was conducted during June of 2002 at the Boulder Atmospheric Observatory (BAO) in Erie, Colorado. For the experiment, comparative measurements were collected using two vertically pointing, collocated radars. One was a UHF BLR that had been configured to operate in a RIM mode. The other was an S-Band frequency-modulated continuous wave (FMCW) radar.

Four frequencies were selected for the RIM measurements using the BLR. These were 914.0, 914.33, 915.33, and 916.0 MHz. The motivation for using a logarithmic frequency spacing as opposed to a linear spacing is discussed in Chilson et al. [2003]. The four frequencies were generated by mixing a switchable local oscillator (LO) with a 60 MHz signal from a coherent oscillator (COHO). The radar configuration was similar to that shown in Figure 1 of Chilson [2004]. The transmitted pulse width was 1.4 μs, which corresponds to a nominal range resolution of 210 m. The returned signal was sampled at 700 ns, that is, every 105 m in range.

The FMCW radar used for the validation experiment has a center frequency of 2.9 GHz and a bandwidth up to 200 MHz. It is capable of probing the boundary layer with a range resolution on the order of 1 m. For this particular experiment, a 2-m range resolution was selected and data were collected up to 2 km above ground level (AGL). Unfortunately, the radar is not capable of making Doppler wind measurements. A description of the radar can be found in Eaton et al. [1995].

4 Results

An example of the results from the comparison are given in Figure 1. The middle and upper panels depict range-time-intensity (RTI) plots of the range corrected signal-to-noise ratio (SNR) calculated from the wind profiler data with and without RIM processing, respectively. That is, the *same* radar observations are shown in both panels; however, the SNR data in upper panels were calculated using "conventional" radar signal processing, whereas the SNR data in lower panels were calculated RIM (see Chilson et al. [2003] for more details). The lower panel shows the RTI plots of C_n^2 obtained from the FMCW radar.

The quantity C_n^2 shown in Figure 1 is the refractive index structure parameter. It is related to the radar volume reflectivity through the equation

$$\eta = 0.38 C_n^2 \lambda^{-1/3}, \tag{2}$$

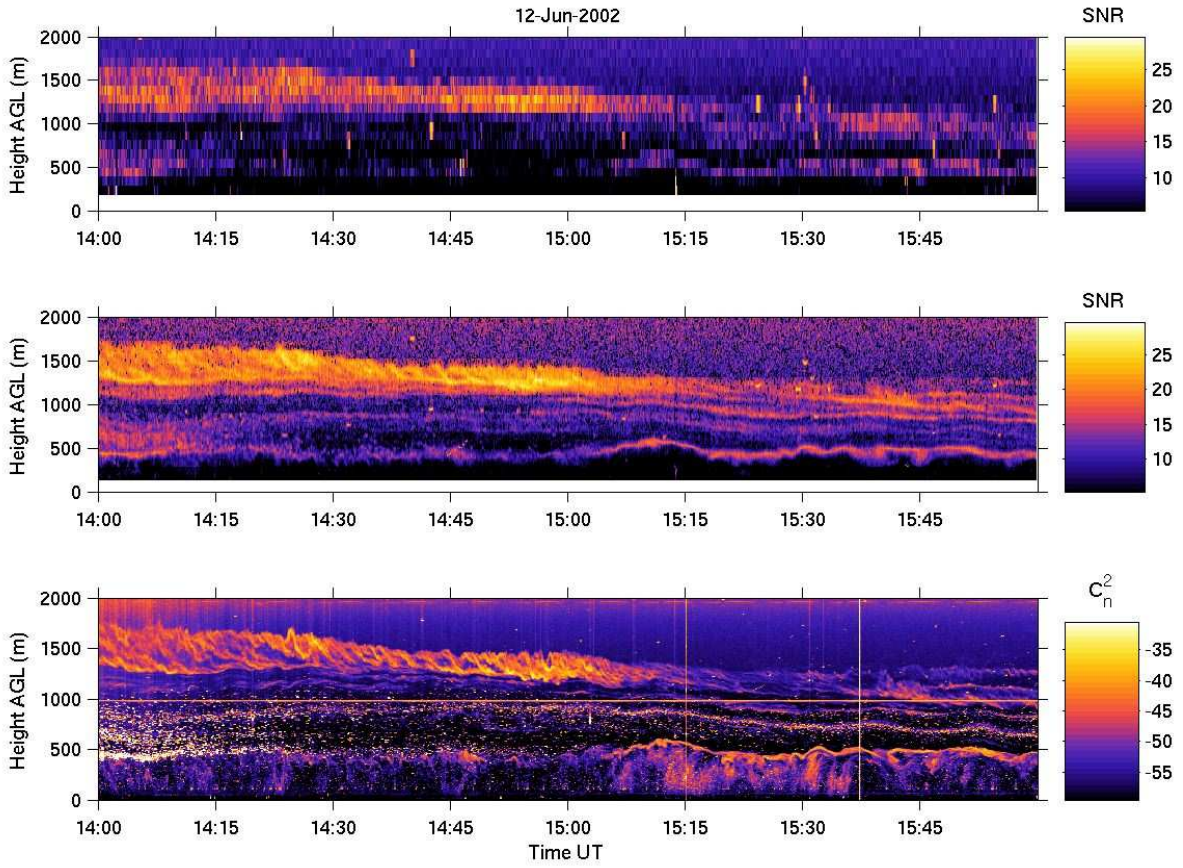

Figure 1: .Results from a recent range imaging validation experiment. The middle and upper panels show RTI plots of the range corrected signal-to-noise ratio (SNR) calculated from BLR data *with* and *without* RIM processing, respectively. The lower panel shows the RTI plots of C_n^2 obtained from the FMCW radar. See text for details.

where λ is the radar wavelength [e.g., Röttger and Larsen, 1990, pg 240]. Furthermore, assuming that the signal noise is constant with height, then the the range corrected power is directly proportional to η. Therefore, C_n^2 should be directly proportional to the range corrected backscattered power.

Clearly the RIM processed data shown in Figure 1 reveal much more detail than would have been observed using conventional signal processing. The small scale features are completely obscured in the conventionally processed data. Certain differences between the BLR and FMCW data are expected since the operating frequencies are not the same (915 MHz and 2.9 GHz), the instruments are separated by roughly 100 m, and the FMCW radar has a resolution of 2 m (compared to the nominal resolution of 210 m for the wind profiler). Bearing these differences in mind, the agreement between the RIM processed data and the FMCW results is very good and indicate that RIM experiments are well suited for BLR measurements of the atmospheric boundary layer.

Figure 2 has been produced in order to better illustrate the ability of RIM to probe inside of the radar sampling volume. This figure presents the same results as given in Figure 1, except

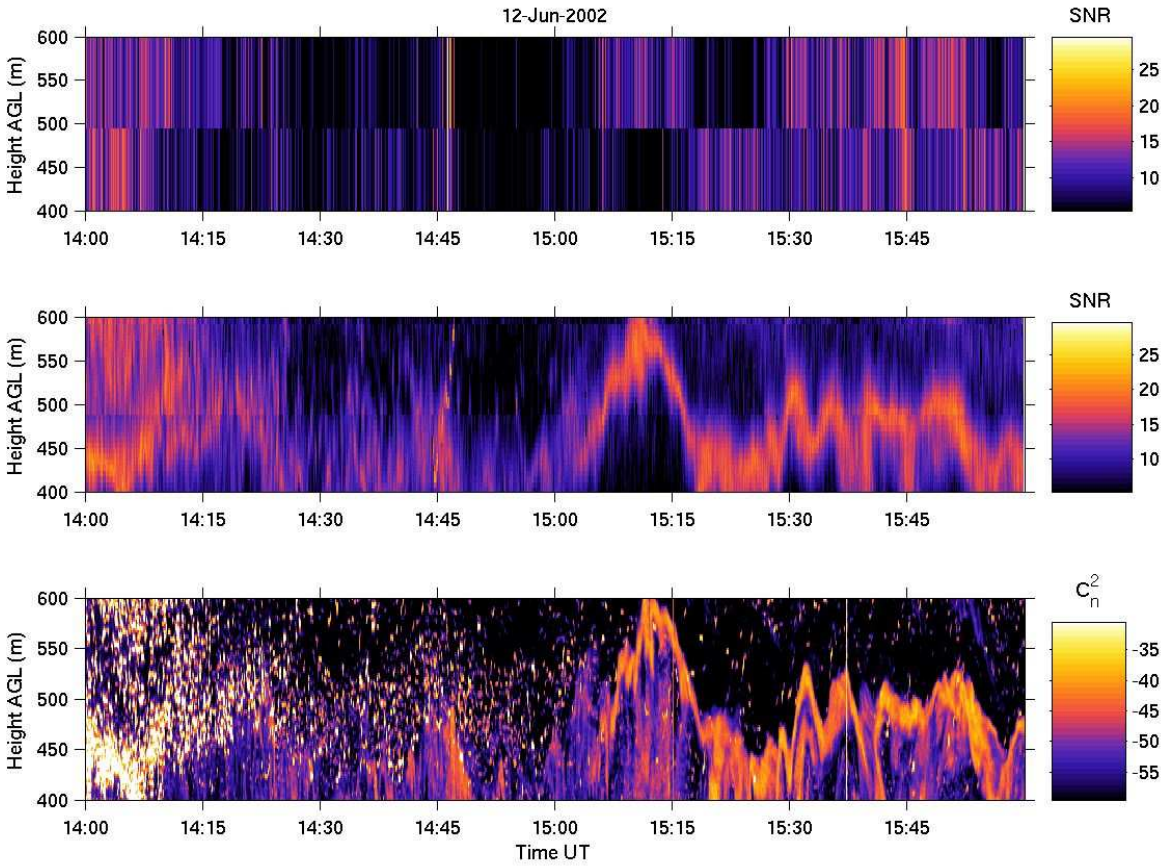

Figure 2: The same as Figure 1 except that only heights ranging from 400 m to 600 m AGL are shown..

that only heights ranging from 400 m to 600 m above ground level are shown. The height range of 200 m roughly spans two sampling volumes as defined by the 700 ns sample spacings. The temporal evolution (height and thickness) of the layer of enhanced echo power (C_n^2) as revealed in the FMCW radar data are well reproduced in the middle panel of Figure 2. Note that the speckles in the FMCW radar data are echos from migrating miller moths.

The data presented so far not only illustrate the effectiveness of RIM, but also the complexity of the dynamic structures present in the daytime convective boundary layer (CBL). As a second example, the subsequent 2-h data interval is shown in Figure 3. Here the CBL is becoming more well developed and the structures more complex. For this 2-h interval, the vertical wind measurements from both the conventional and RIM radar signal processing are also shown in 4. Note that here no comparative data from the FMCW radar exist. It can be seen however, that the RIM-generated wind data are similar to those from the conventional processing, but with more structured and detailed.

5 Discussion

Many structures exist in the atmospheric boundary layer that have spatial scales that are too small to be adequately resolved using conventional profiling radars. However, the ability to accurately measure and monitor these structures

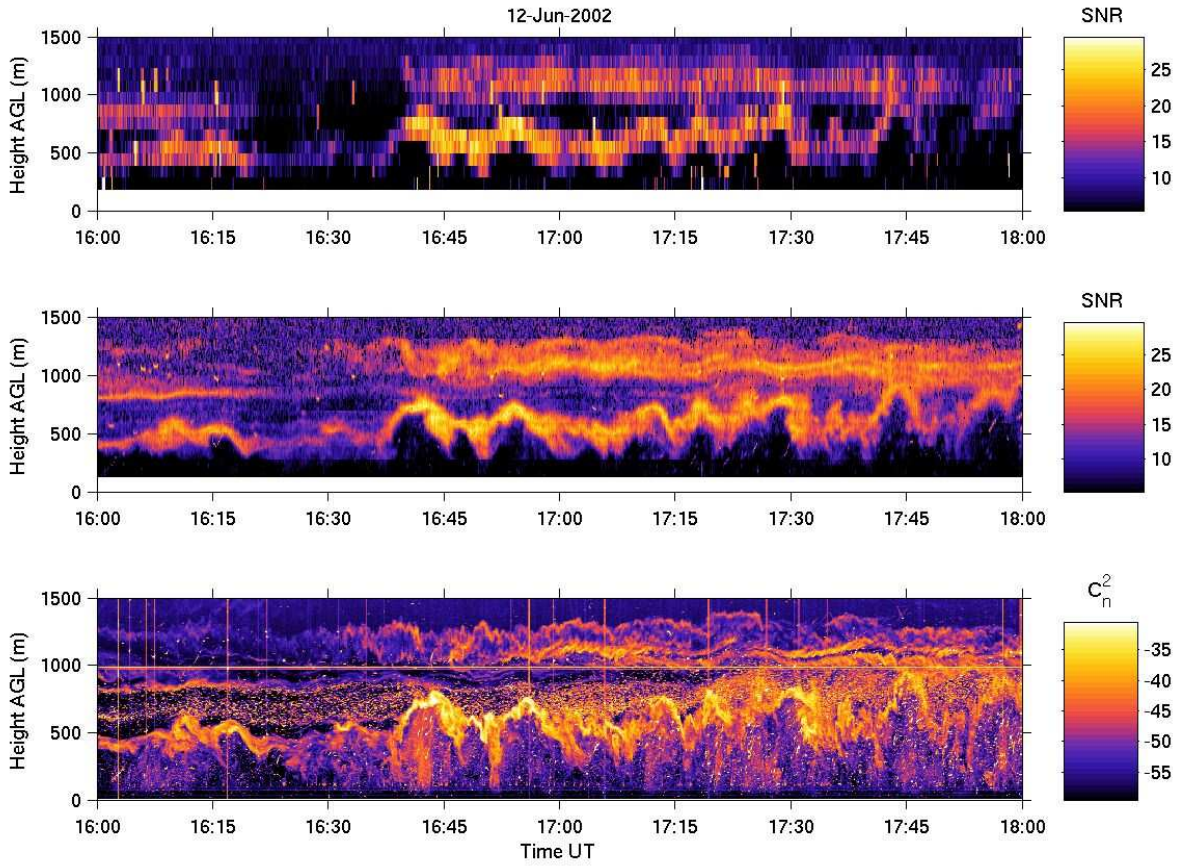

Figure 3: The same as Figure 1 except that the time window extends from 16:00 to 18:00 UT.

can be extremely important. For example, the convective boundary layer (CBL) is topped by the entrainment zone, where stable stratification inhibits vertical mixing, and vertical gradients of averaged meteorological fields become comparatively large. The entrainment zone is often identified as the interfacial layer. In many CBL cases, the entrainment zone is collocated with the region of maximum gradients in the potential temperature profile – the so-called capping inversion layer, the height of which is denoted by z_i.

Profiles of many quantities within the CBL can be scaled with inversion height z_i [Deardorff, 1970], which is often taken as a measure of the CBL depth. These include mean flow parameters (mean wind speed, potential temperature, and specific humidity), turbulent fluxes of momentum, heat, and moisture, and variances of the velocity components and passive scalars. Consequently, an accurate knowledge of z_i is highly relevant for any study of the convective boundary layer structure. RIM can be effectively used to measure such quantities as the CBL depth and the entrainment zone thickness.

The validation of RIM is difficult using in-situ measurements such as rawinsondes or instrumented towers. Given the complex structure of the boundary layer, it is impossible to know if a layer detected by the rawinsonde has the same height as seen by the radar. Also, the rawinsonde may have been carried far away from the radar sampling volume by the time it obtains an altitude that can be detected by the radar. Meteo-

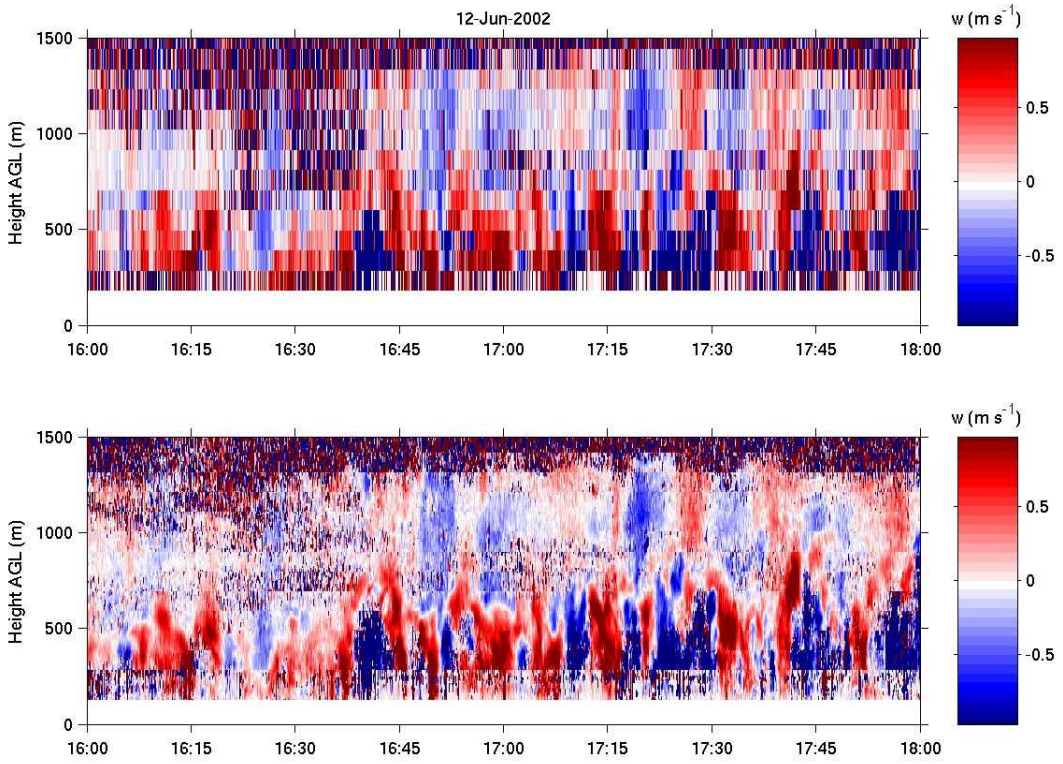

Figure 4: Vertical velocities calculated for the data corresponding to those shown in Figure 3.

rological towers are seen as clutter targets if they are too near to the radar. Also, most meteorological towers are well below the lowest sampling volume of the radar. Therefore, in this study, the RIM echo power has been compared against data obtained with an FMCW radar. Considering the differences in sampling volumes and radar frequencies, the range corrected RIM echo powers from the BLR agree remarkably well with the values of C_n^2 measured with the FMCW radar. The FMCW radar used for the comparison was not capable of making Doppler measurements, so it was not possible to validate the RIM velocities.

Acknowledgments

This work has been supported in part by Vaisala Inc. The authors are gratefully acknowledge the inputs and assistance provided by Dr. Richard Strauch during the course of this study.

References

Angevine, W. M., 1999: Entrainment results with advection and case studies from the Flatland boundary layer experiments. *J. Geophys. Res.*, **104**, 30947–30963.

Angevine, W. M., A. B. White, and S. K. Avery, 1994: Boundary-layer depth and entrainment zone characterization with a boundary-layer profiler. *Boundary-Layer Meteor.*, **68**, 375–385.

Balsley, B. B., and K. Gage, 1982: On the use of radars for operational profiling. *Bull. Amer. Meteor. Soc.*, **63**, 1009–1018.

Chau, J. L., and R. F. Woodman, 2001: Three-dimensional coherent radar imaging at Jicamarca: Comparison of different inversion techniques. *J. Atmos. Sol. Terr. Phys.*, **63**, 253–261.

Chilson, P. B., 2004: The retrieval and validation of Doppler velocity estimates from range imaging. *J. Atmos. Ocean. Tech.*, **21**(7), 1033–1043.

Chilson, P. B., T.-Y. Yu, R. G. Strauch, A. Muschinski, and R. D. Palmer, 2003: Implementation and validation of range imaging on a UHF radar wind profiler. *J. Atmos. Ocean. Tech.*, **20**(7), 987–996.

Cohn, S. A., and W. M. Angevine, 2000: Boundary level height and entrainment zone thickness measured by lidars and wind-profiling radars. *J. Appl. Meteorol.*, **39**(1233-1247).

Dabberdt, W. F., G. L. Frederick, R. M. Hardesty, W. C. Lee, and K. Underwood, 2004: Advances in meteorological instrumentation for air quality and emergency resposnse. *Meteor. Atm. Phys.*, **87**, 57–88.

Deardorff, J. W., 1970: Preliminary results from numerical integration of the unstable boundary layer. *J. Atmos. Sci.*, **27**, 1209–1211.

Eaton, F. D., S. A. McLaughlin, and J. R. Hines, 1995: A new frequency-modulated continuous wave radar for studying planetary boundary layer morphology. *Radio Sci.*, **30**(1), 75–88.

Ecklund, W. L., K. S. Gage, and C. R. Williams, 1995: Tropical precipitation studies using a 915-MHz wind profiler. *Radio Sci.*, **30**, 1055–1064.

Gage, K. S., C. R. Williams, and W. L. Ecklund, 1994: UHF wind profilers: A new tool for diagnosing and classifying tropical cloud systems. *Bull. Amer. Meteor. Soc.*, **75**, 2289–2294.

Grimsdell, A. W., and W. M. Angevine, 2002: Observations of the afternoon transition of the convective boundary layer. *J. Appl. Meteorol.*, **41**, 3–11.

Hysell, D. L., 1996: Radar imaging of equatorial F region irregularities with maximum entropy interferometry. *Radio Sci.*, **31**, 1567–1578.

Luce, H., M. Yamamoto, S. Fukao, D. Helal, and M. Crochet, 2001: A frequency domain radar interferometric imaging (FII) technique based on high resolution methods. *J. Atmos. Sol. Terr. Phys.*, **63**, 201–214.

Palmer, R. D., S. Gopalam, T.-Y. Yu, and S. Fukao, 1998: Coherent radar imaging using Capon's method. *Radio Sci.*, **33**(6), 1585–1589.

Palmer, R. D., T.-Y. Yu, and P. B. Chilson, 1999: Range imaging using frequency diversity. *Radio Sci.*, **34**(6), 1485–1496.

Rogers, R. R., W. L. Ecklund, D. A. Carter, K. S. Gage, and S. A. Ethier, 1993: Research applications of a boundary-layer wind profiler. *Bull. Amer. Meteor. Soc.*, **74**(4), 567–580.

Röttger, J., and M. F. Larsen, 1990: UHF/VHF radar techniques for atmospheric research and wind profiler applications. in D. Atlas, editor, *Radar in Meteorology*, pp. 235–286. Am. Meteorol. Soc., Boston, Mass.

Smaïni, L., H. Luce, M. Crochet, and S. Fukao, 2002: An improved high-resolution processing method for a frequency domain interferometric FII technique. *J. Atmos. Ocean. Tech.*, **19**(6), 954–966.

Wilczak, J. M., E. E. Gossard, W. D. Neff, and W. L. Eberhard, 1996: Ground-based remote sensing of the atmospheric boundary layer: 25 years of progress. *Boundary-Layer Meteor.*, **78**, 321–349.

Woodman, R. F., 1997: Coherent radar imaging: Signal processing and statistical properties. *Radio Sci.*, **32**, 2372–2391.

Yu, T.-Y., and R. D. Palmer, 2001: Atmospheric radar imaging using spatial and frequency diversity. *Radio Sci.*, **36**(6), 1493–1504.